



Article

Natural Clay Minerals as Potential Arsenic Sorbents from Contaminated Groundwater: Equilibrium and Kinetic Studies

Ambrin Rehman ¹, Shah Rukh ^{1,*}, Samha Al Ayoubi ², Seema Anjum Khattak ¹, Ayaz Mehmood ³, Liaquat Ali ¹, Ahmad Khan ⁴, Kouser Majeed Malik ⁵, Abdul Qayyum ⁶ and Hikmat Salam ¹

¹ National Centre of Excellence in Geology, University of Peshawar, Peshawar 25130, Pakistan; rehmanambrin94@gmail.com (A.R.); s_anjum@uop.edu.pk (S.A.K.); liaquat.nceg@uop.edu.pk (L.A.); hikmatsalam@uop.edu.pk (H.S.)

² College of Humanities and Sciences, Prince Sultan University, Rafha Street, Riyadh 11586, Saudi Arabia; sayoubi@psu.edu.sa

³ Department of Soil and Climate Sciences, The University of Haripur, Haripur 22620, Pakistan; ayaz.gill@uoh.edu.pk

⁴ Institute of Soil and Environmental Sciences, Pir Mehr Ali Shah Arid Agriculture University Rawalpindi, Rawalpindi 46300, Pakistan; ahmadk78@gmail.com

⁵ Soil and Water Testing Laboratory for Research, Rawalpindi 46300, Pakistan; kousermajeed9@gmail.com

⁶ Department of Agronomy, The University of Haripur, Haripur 22620, Pakistan; aqayyum@uoh.edu.pk

* Correspondence: shahrukh.nceg@uop.edu.pk; Tel.: +92-336-5132003

Abstract: Arsenic (As) contaminated groundwater is a worldwide concern due to its chronic effects on human health. The objectives of the study were to evaluate natural inexpensive raw laterite (RL) and kaolinite (RK) for their potential use as As sorbents and to understand the As sorption on laterite and kaolinite by employing sorption and kinetic models. Raw laterite and RK were tested for EC, pH, XRF and CEC as basic parameters. Batch sorption and kinetic experiments data were fitted in the sorption (Langmuir and Freundlich) model and kinetic (pseudo-first and pseudo-second order) reaction equations, respectively. Morphological and structural changes were observed in RL and RK samples before and after As saturation by employing FTIR and SEM. The major constituent in RL was Fe and Al oxides while in RK major oxides were silica and Al. The Freundlich sorption model well explained the experimental data, indicating a greater sorption capacity of RL on a hetero-layered surface compared to RK. The kinetic reaction equations showed that equilibrium was achieved after a contact time of 240 min and the adsorption was chemisorption in nature. The RL and RK were found to be effective sorbents for As removal, however, RL showed maximum As adsorption and thus superior in comparison with RK. Structural and morphological characterization reveals the role of Fe and Al oxides in the case of RL, and Al oxides in the case of RK, in the adsorption of As. Hence this study concludes that these naturally occurring inexpensive resources can be used as sorbent agents for As-contaminated drinking water treatment.

Keywords: sorption kinetics; isotherms studies; natural sorbents; arsenic contamination

Citation: Rehman, A.; Rukh, S.; Ayoubi, S.A.; Khattak, S.A.; Mehmood, A.; Ali, L.; Khan, A.; Malik, K.M.; Qayyum, A.; Salam, H. Natural Clay Minerals as Potential Arsenic Sorbents from Contaminated Groundwater: Equilibrium and Kinetic Studies. *Int. J. Environ. Res. Public Health* **2022**, *19*, 16292. <https://doi.org/10.3390/ijerph192316292>

Academic Editors: Marcello Iriti, Luigi Falciola and Valeria Ancona

Received: 2 November 2022

Accepted: 25 November 2022

Published: 5 December 2022

Publisher's Note: MDPI stays neutral with regard to jurisdictional claims in published maps and institutional affiliations.



Copyright: © 2022 by the authors. Licensee MDPI, Basel, Switzerland. This article is an open access article distributed under the terms and conditions of the Creative Commons Attribution (CC BY) license (<https://creativecommons.org/licenses/by/4.0/>).

1. Introduction

Arsenic (As) is carcinogenic and causes severe health threats to humans [1]. It occurs naturally as a metalloid in the environment and ranges from 0.5 to 2.5 mg kg⁻¹ in most of the rocks but some sediments and fine grain phosphites have high proportions [2]. Inorganic As exists as oxides of sulfur, oxygen, iron, and in trivalent (arsenite, AsIII) and pentavalent (arsenate, AsV) oxidation states [3,4]. The AsV occurrence is dominant in natural ecosystems while AsIII prevails in reduced conditions, though both are toxic and cause acute and chronic toxicity in humans [5].

Arsenic is released into the environment through mineral dissolution, chemical decomposition, weathering of rocks and soils and volcanic activity [6]. Minerals associated

with iron (arsenopyrite (FeAsS)), sulfide ores (ruby sulfur (AsS) and orpiment (As_2S_3)) are major As release sources [7]. Industrial and mining processes such as dyes and colors, wood preservatives, cement works, electronics and glassware production, disinfectants and pesticides, ores and metals treatment, and cotton drying agents are also key contributors to As release into the environment [8–10].

Natural and anthropogenic activities have caused As contamination in groundwater [11]. The “Arsenic Problem” first came to light in the mid-1990s in Bangladesh; since then various regions of the world including Vietnam, India, China, Argentina, Chile, Mexico, Hungary and many parts of the USA have been reported to have high levels of As in drinking water [12] posing a direct threat to more than tens of millions of people across the globe [13]. About 50 to 60 million people in the Indus plain of Pakistan, with hot spots around Lahore and Hyderabad, are exposed to As-contaminated drinking water [14]. Muzaffargarh, a district of Southern Punjab, Pakistan has been reported with very high As toxicity of $906 \mu\text{g L}^{-1}$ in groundwater [15] which is beyond the permissible limit of $50 \mu\text{g L}^{-1}$ for drinking water [16]. The maximum human tolerance level in drinking water for As concentration is $10\text{--}50 \mu\text{g L}^{-1}$, however, different countries have adopted the WHO standard of $10 \mu\text{g L}^{-1}$ [17,18]. Exposure to inorganic As ($>50 \mu\text{g L}^{-1}$) results in deleterious health effects [19,20] and causes arsenicosis [21], skin, lung, bladder, and kidney cancers and acute myocardial infection [22].

Several known treatment mechanisms for the efficient removal of As from water are coagulation [23–27], softening [28], anion exchange and reverse osmosis [29]. These methods have economic limitations, though, and the adsorption technique is an economic and suitable method [30] for As decontamination using laterite [31,32] and clay minerals [33].

Naturally occurring minerals both in the raw and modified form are widely used for the removal of inorganic and organic pollutants from contaminated water [34–36]. Laterite mainly consists of mineral assemblages of hematite, gibbsite, kaolinite mineral, quartz, and a small amount of goethite [37]. The adsorption mechanism of As forms by laterite and lateritic soils of India has been extensively studied [6,31,38–40] and their adsorption capacities were found comparable with many other synthetic adsorbents [41–43]. The studies showed AsIII bond formation with laterite involved both ion exchange and ligand exchange mechanisms [6]. However, in the case of laterite soil, AsIII adsorbed through physisorption and AsV through an ion exchange mechanism [40]. In another study, laterite obtained from Vietnam was used as sorbent material for AsV and concluded that the sorption process was multilayer, physical, reversible, and engaged Van Der Waals forces [44]. Clay minerals can remove organic and inorganic substances from aqueous environments [45]. Kaolinite is a 1:1 clay mineral group of alumina silicates ($\text{Al}_2\text{O}_3(\text{SiO}_2)_2(\text{H}_2\text{O})_2$) characterized by fine particle size, chemical inertness, and a platy structure [46]. Surface-modified kaolinite with a fluoralkylsilane agent showed excellent performance of 100% As rejection even at 1000 mg L^{-1} concentration in an aqueous solution [47]. Among other cheap materials such as fly ash, dolomite and apatite powder, kaolin clay is preferred due to its appropriate pore-forming ability which is important for the fabrication of stable micro-filtration-range inorganic membranes at a lower cost [48]. The physical nature of the As adsorption process with monolayer formation of sorbate on solid surfaces of ZnO nanoparticles-coated kaolin was observed [49]. The study also revealed that As kinetic adsorption on synthesized adsorbent followed a pseudo-second-order equation, indicating internal and external mass transfer simultaneously. Kaolinite, a cheap natural material commercially available in the market, has been found effective for the removal of Pb^{+2} , Ni^{+2} , Cd^{+2} and Cr^{+6} ions from drinking water [50]. The metals showed multilayer adsorption on surfaces having heterogeneous binding sites and followed second-order adsorption kinetics.

Laterite and kaolinite deposits are widely reported across the country with varied geological settings and formations [51].

Third world countries like Pakistan cannot afford expensive treatment systems or bottled water and thus need an affordable low-tech solution for safe drinking water.

Identification of indigenous, low-cost clay materials has limited their use in household filter systems. Local deposits of laterite and kaolinite-rich clays can be a cheaper source for As removal from drinking water. The present study aimed to identify an effective natural indigenous raw clay material (kaolinite and/or laterite) for As removal from contaminated drinking water. The specific objectives of this study were to determine As sorption capacity of laterite and kaolinite for their potential use as sorbents and to understand the sorption kinetics of As on raw laterite and raw kaolinite.

2. Materials and Methods

2.1. Sample Collection and Preparation

Laterite and kaolinite samples were collected from known deposits located in Khyber Pakhtunkhwa (Figure 1). Kaolinite samples were collected from the low hilly parts of Taghma, Tarkano, and the Matta area of Swat, Khyber Pakhtunkhwa. These Kaolin deposits at Swat occur within Kohistan ortho-amphibolites of Cretaceous age. The ortho-amphibolites contain felsic zones and leucocratic dikes that constitute the host rocks of Kaolin. They are part of the Cretaceous Kohistan island arc terrane [52]. The laterite samples were collected from the Kakul Tatta Pani area of Abbottabad district, Khyber Pakhtunkhwa. Laterite deposits in the Abbottabad region are hosted in the Abbottabad Formation of the Cambrian age [53,54]. A total of five different sites were sampled, namely, Tarkano-1, Tarkano-2, Taghma-1, Taghma-2 and Matta, for kaolinite, and HB-6, HB-7, HB-9, HB-10 and HB-12 for laterite. The freshly exposed surface was sampled manually by removing surface debris from the exposed deposits of kaolinite and laterite and stored in zip-lock plastic bags with proper labels. All samples were shifted to the geochemistry laboratory of NCE in Geology and were dried at room temperature. The samples were ground to pass through a 200 μm mesh size before further morphological and experimental analysis.

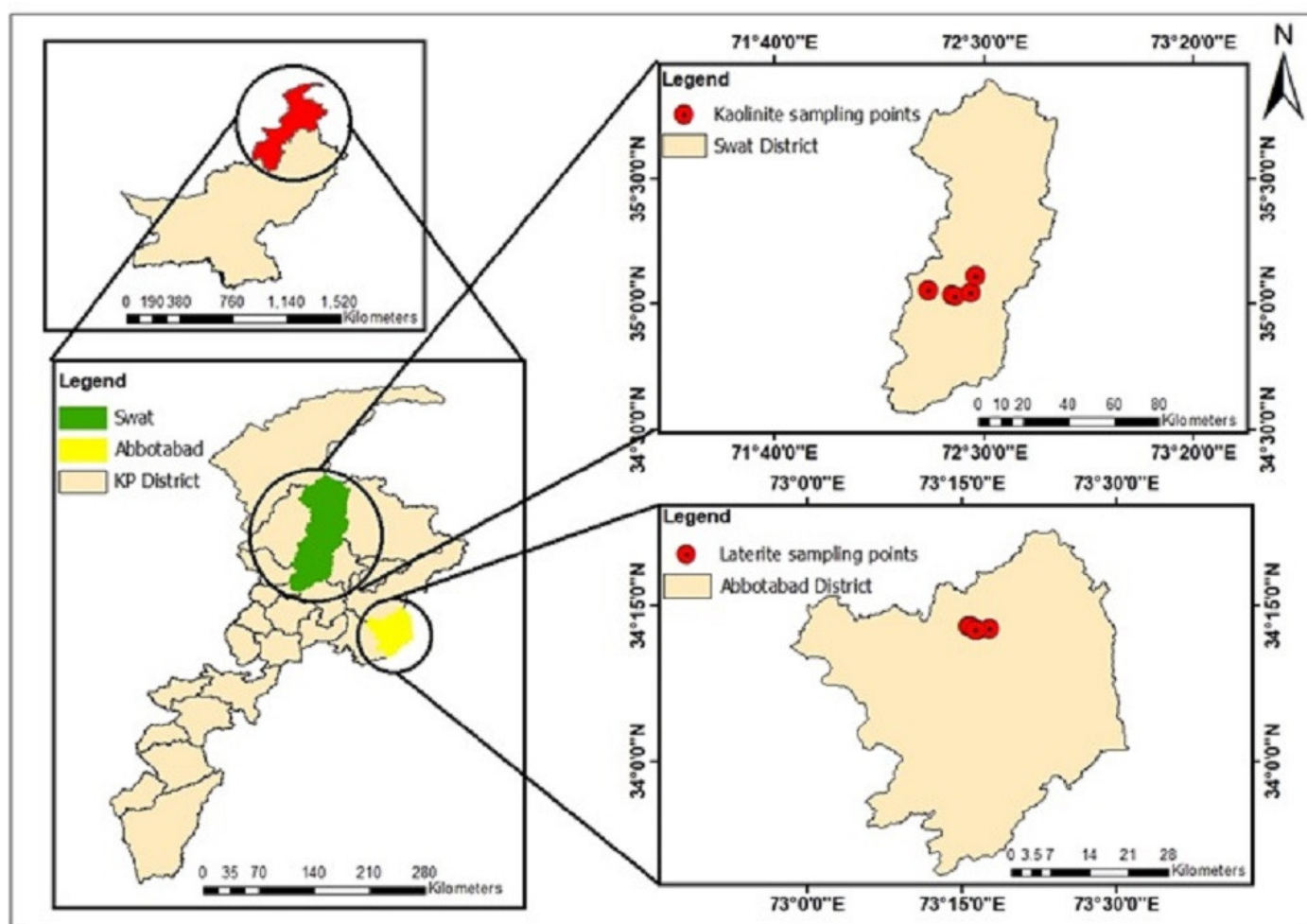


Figure 1. Map showing the study area and Kaolinite and Laterite sampling points in the Swat and Abbottabad districts, Khyber Pakhtunkhwa, Pakistan.

2.2. Basic Properties

The pH of each laterite and kaolinite sample was measured by making a 1:2.5 sample water suspension [55]. A twenty g sample was taken in 50 mL water, stirred and allowed to stand for 30 min. After 30 min, the pH was measured using a C931 Electrochemical analyzer made by Consort (Turnhout, Belgium) pre-calibrated with buffers 4 and 7. For EC, a 1:5 sample and water suspension was prepared [56]. A five g sample was taken in a beaker with 25 mL water, stirred and allowed to stand for 30 min before taking a reading with a C931 Electrochemical analyzer. Before taking a reading, the instrument was calibrated with a reference solution of 0.01 M KCl, with a conductivity of 1413 $\mu\text{S cm}^{-1}$.

Laterite and kaolinite clays were analyzed for cation exchange capacity (CEC) by saturating the samples with sodium cations [57]. A five g sample was taken in 50 mL centrifuge tubes and 30 mL of $\text{C}_2\text{H}_3\text{NaO}_2$ (1M) solution was added, shaken for 5 min, followed by centrifugation at 5000 \times g rpm for 15 min, repeated three times, and the supernatant was discarded. The sample was then washed with 30 mL of 95% ethanol by shaking and centrifugation three times. Then 1 M $\text{C}_2\text{H}_7\text{NO}_2$ (30 mL) was added to the suspension, centrifuged after 5 min shaking, repeated three times, and the decant was collected in a volumetric flask, and the volume was made up to 100 mL with $\text{C}_2\text{H}_7\text{NO}_2$. The concentration of Na was measured in the collected supernatant using a flame photometer. The following equation was used to calculate the meq of Na/100 g.

$$\text{meq of Na/100 g sample} = \text{emission reading (R meq/L)} \times \frac{100 \text{ mL}}{1000 \text{ mL}} \times \frac{100 \text{ g}}{\text{Wt. of sample (g)}} = \frac{\text{R} \times 10}{\text{Wt. of sample (g)}}$$

where R is the meq/L of Na as determined by the flame photometer. The displaced Na is the measure of the CEC of the sample.

The elemental composition of selected laterite and kaolinite clays was determined by X-ray fluorescence. Powdered laterite and kaolinite clays were infused in pellet form with 4–5 drops of epoxy glue. An amount of 0.5 g of each of the clays was used to prepare pellet of 199 mm diameter under a 10-tonne hydraulic press. Each pellet was separately placed on the holder of the specimen chamber and bombarded with X-rays emitted from the X-ray tube window.

2.3. Adsorption of As on Laterite and Kaolinite

2.3.1. Batch Sorption Experiments

Batch sorption studies were carried out for sorption isotherms and the data were fitted in the Langmuir and Freundlich equations to model parameters. Triplicate 3 g samples of laterite, and kaolinite were equilibrated with 30 mL of 0.01 M KNO_3 solution containing 0, 0.5, 2, 10, 30, 50, 70 and 100 mg L^{-1} of As using Na_2AsO_4 . The suspension was shaken for 48 h at 25 °C and centrifuged at 5000× g rpm for 15 min. The supernatant was filtered through a 0.45-micron cellulose membrane, acidified and analyzed for the As solution concentration using atomic absorption equipped with hydride vapor generation (HVG-AAS). The difference in applied concentration and equilibrium As solution concentration (C_w) was taken as the sorbed amount. The maximum adsorption capacity (b) and surface binding strength (K) were calculated by fitting the data in the Langmuir model (Equation (1)) [58–60].

$$X = \frac{bKC_w}{1+KC_w} \quad (1)$$

The linear form of the Langmuir model is

$$\frac{C_w}{X/m} = \frac{1}{Kb} + \frac{C_w}{b} \quad (2)$$

where C_w is the equilibrium concentration, X is the adsorbed concentration, m is the mass of soil, K is the surface binding strength, and b is the maximum adsorption capacity.

The adsorption isotherm was also fitted to the Freundlich equation [61]:

$$\frac{X}{m} = k_f C_w^{\frac{1}{\beta}} \quad (3)$$

or rearranged in the linear form:

$$\log X/m = \log k_f + \frac{1}{\beta} \log C_w \quad (4)$$

where X/m is the equilibrium concentration adsorbed by the soil (mg kg^{-1}), C_w is the equilibrium concentration in solution (mg L^{-1}), β is an adsorption exponent related to adsorption intensity and k_f is the Freundlich adsorption coefficient (L kg^{-1}) related to maximum adsorption capacity. A plot of $\log X/m$ versus $\log C_w$ was fitted using linear regression; β was found by the reciprocal of the slope of the regression line. The intercept of this regression line yielded k_f .

2.3.2. Adsorption Kinetics of As

In kinetic experiments, 30 mL As solution having a concentration of 0.5 mg L^{-1} was used with 3 g of laterite and kaolinite samples. The suspension was shaken at 120 rpm for specific time intervals i.e., 0, 120, 240, 480 and 720 min. Immediately, after shaking the suspension was centrifuged at 5000× g rpm for 5 min and the supernatant was filtered through a 0.45-micron membrane and filtrates were stored at 4 °C after acidifying till analysis. The kinetic experiment data were fitted to the Pseudo-first-order kinetic equation [62] using the Origin 8.5 software.

$$q_t = q_e (1 - e^{-k_1 t}) \quad (5)$$

where q_t is the sorbed amount (mg g^{-1}) at time t (min), q_e is the sorbed amount (mg g^{-1}) at equilibrium, and k_1 is the pseudo-first-order rate constant (min^{-1}). A non-linear fit to the above-mentioned equation was employed using the Box-Lucas function which yields q_e as the intercept and k_1 as the slope. A fitting to a pseudo-first-order kinetic model indicates that the reaction-limiting step is governed mainly by the physisorption. This model suggests that the sorption rate is proportional to the difference between the amount of adsorbed sorbate at time t and the amount of adsorbed sorbate at equilibrium. Eventually, the sorption is reversible and reaches equilibrium.

The kinetic experiment data was also fitted to the pseudo-second-order kinetic equation [63].

$$q_t = \frac{q_e^2 \cdot k_2 \cdot t}{1 + q_e \cdot k_2 \cdot t} \quad (6)$$

where q_t is the capacity (mg g^{-1}) at the time (min), q_e is the capacity (mg g^{-1}) at equilibrium and k_2 is the pseudo-second-order rate constant ($\text{mg g}^{-1} \text{min}^{-1}$). This equation was also solved by employing the Origin 8.5 software. The q_e and k_2 were estimated by keeping t as the independent variable and q_t as the dependent variable. This model suggests that the adsorption capacity is proportional to the active sites occupied by the sorbate. A fitting to the pseudo-second-order kinetic model indicates that the reaction is governed principally by chemisorption as the limiting step.

The solution concentration for both batch sorption and kinetic adsorption experiments was maintained at 7 to mimic the real groundwater. The WHO recommends a pH range of about 6.5 or higher for drinking water [18]. Good quality water usually has pH values in the range of 6.5 and 8.5.

After the sorption and kinetic experiments, one sample each from laterite and kaolinite was selected for the FTIR and SEM-EDX analysis. For understanding the mechanism of adsorption, the changes in each selected laterite and kaolinite sample before adsorption and after adsorption was compared.

2.4. Post-Adsorption Studies

2.4.1. ATR-FTIR

The structural composition of laterite and kaolinite was determined by Fourier transform infrared spectroscopy (FTIR) by making a KBr pellet. Two hundred mg of the homogenized mixture of powdered sample and KBr (1:110) was pressed to form a die under vacuum. The pellet was left in a desiccator overnight and scanned between 400–4000 cm^{-1} using a Shimadzu FTIR instrument, Kyoto, Japan [64].

2.4.2. SEM-EDX

The morphology of laterites and kaolinite was studied through scanning electron microscopy (SEM) coupled with energy dispersive X-ray (EDX) for elemental analysis. The powdered samples were gold-coated by evaporation under a high vacuum using a gold coater.

2.5. Arsenic Determination

Total As concentration of the aliquots of kinetic and batch sorption experiments were determined using a Shimadzu AA-6300 atomic absorption spectrophotometer coupled with Shimadzu HVG-1 hydride vapor [65]. The absorption was measured at 193.7 nm wavelength using a slit-width of 0.7 nm, a lamp power supply of 7W, and an air/acetylene flame. In the hydride generation assembly, arsine (AsH_3) produced by a premix of 0.4% NaBH_4 and 0.5% NaOH solutions, was mixed with 5 M HCl in the mixing chamber [66]. The acid and the premix of NaBH_4 and NaOH were, separately, pumped at a rate of one

mL min⁻¹ using a peristaltic pump to the gas–liquid separator chamber from where the AsH₃ gas was carried to the flame by N₂ gas at 0.32 MPa. The detection limit was 2.42 µg L⁻¹ as determined by analyzing 10 blanks and calculating the standard deviation ($\sigma = 0.26$). The detection limit was a mean of 10 blank samples plus three times the standard deviation.

3. Results and Discussion

Raw laterite and kaolinite samples were characterized for their basic properties (pH, EC and CEC) and elemental composition using XRF. The As sorption potential of raw laterite and kaolinite was determined by batch and kinetic studies. Langmuir and Freundlich equations were used to fit the batch sorption experimental data and the models' regression equations were employed to calculate adsorption parameters. Equilibrium data were fitted to pseudo-first- and pseudo-second-order equations. One sample each of laterite and kaolinite was selected for further morphological studies (SEM and FTIR) for understanding the sorption mechanism of As on to laterite and kaolinite. The detailed results are explained below.

3.1. Basic Properties

The results presented in Table 1 show that the pH of the laterite and kaolinite samples were in the acidic-to-near-neutral range. The laterite samples' pH ranged from 5.9 to 7.1, with the lowest pH of 5.9 observed in HB-10, whereas the pH of the kaolinite samples was in the range of 6.5 to 7.5, with the highest pH observed in Taghma-1. The pH values below 7 may indicate the presence of hydrogen ions on the exchange sites which results in more anion exchange capacity. The increase in the pH values results in lower hydrogen ions on exchange sites and inflated CEC values. Our results are in agreement with Ko [67], who observed most of the laterite samples' pH values in the acidic range. Maiti et al. [31] reported laterite pH values in the range of 7.0–7.2. Similarly, Li and Xu [68] found the pH of kaolinite in the acidic (5.3) range, which was slightly lower than the pH of the kaolinite used in this study. Moreover, most samples had pH values in the acidic range.

Table 1. Characteristics of the raw laterite and kaolinite samples.

Sample	Fe ₂ O ₃ %	Al ₂ O ₃ %	SiO ₂ %	CaO %	K ₂ O %	P ₂ O ₅ %	TiO ₂	Mn ₂ O ₃	pH	EC mS/cm	CEC meq/100 g
Laterite											
HB-10	46.27	5.94	2.22	1.58	0.027	6.44	-	0.11	5.9 _(0.5)	3.6 _(0.8)	7.62 _(2.45)
HB-7	45.33	6.38	3.18	3.10	0.02	1.51	-	0.1	6.5 _(0.4)	4.8 _(1.3)	24.95 _(2.44)
HB-9	24.44	12.85	1.69	0.4	0.012	0.41	-	0.05	7.1 _(0.4)	6.2 _(0.7)	15.41 _(6.12)
HB-16	58.14	6.4	3.09	3.07	0.03	0.52	-	0.12	7.1 _(0.3)	6.2 _(1.0)	29.27 _(3.67)
HB-12	49.74	4.47	0.84	20.08	0.16	0.73	-	0.14	6.2 _(0.6)	6.7 _(1.2)	5.42 _(1.22)
Kaolinite											
Tarkano-2	0.6	5.14	10.78	4.71	0.05	0.2	0.2	0.84	6.7 _(0.6)	2.6 _(0.6)	14.55 _(2.45)
Tarkano-1	0.06	6.7	11.52	5.56	0.06	0.13	1.3	0.6	7.1 _(0.3)	1.6 _(0.5)	12.81 _(2.45)
Taghma-2	1.07	9.77	13.91	5.07	0.1	0.13	0.13	0.02	6.9 _(0.3)	3.2 _(0.3)	22.34 _(6.12)
Taghma-1	0.34	3.88	8.01	5.41	0.13	0.2	0.2	0.5	7.5 _(0.2)	4.1 _(0.3)	3.29 _(1.22)
Matta	1.48	5.62	10.42	7.56	0.14	0.11	0.11	0.5	6.5 _(0.5)	2.1 _(0.4)	5.02 _(1.23)

Values in parenthesis indicate standard deviation ($n = 3$).

The optimum pH range for the As (AsV and AsIII) adsorption on natural laterite was found in the range of 4.0 to 7.0, and in this pH range surface active sites are positively charged [6,38] while As forms exist in the form of anions (H₂AsO₄⁻, H₃AsO₃⁻) and are adsorbed onto active sites of the laterite surface. Similarly, maximum adsorption of As was observed in the pH range of 7 to 7.6. on activated alumina [69] and iron oxide-coated sand

[70], as both iron and/or aluminum oxides are responsible for As adsorption on laterite. Adsorption of As on hydrous iron and/or aluminum oxide of natural laterite surface is mainly by ligand exchange, and electrostatic interaction is insignificant [71].

In the case of clay minerals, As adsorption on clay minerals (kaolinite, illite and montmorillonite) was found to be pH dependent [72]. It was noticed that kaolinite adsorption was maximum over the pH range of 2.0 to 5.0, and decreased steadily with an increase in pH. The presence of oxygen atoms on kaolinite surfaces forms positive charge formation in the presence of water, which is responsible for the adsorption of As forms at lower pH. However, at higher pH, kaolinite surfaces become more and more negatively charged, which prevents As adsorption.

The EC of laterite samples varied from 3.6 to 6.7 mS cm⁻¹, while kaolinite samples' EC was observed in the range of 1.6 to 4.1 mS cm⁻¹. Overall, kaolinite samples had lower mean values of EC as compared to the laterite samples. The results show a lower amount of soluble salts in kaolinite as compared to the laterite. Li and Xu [68] reported the EC of kaolinite as 10.1 mS cm⁻¹, which was comparatively high compared to the results of the present study. However, Maiti et al. [39] reported much lower values of 15 µS cm⁻¹ for raw laterite compared to the laterite of the present study.

The CEC of the laterite samples was in the range of 5.42 meq/100 g to 24.95 meq/100 g, while in kaolinite, the CEC was in the range of 3.29 meq/100 g to 22.34 meq/100 g. HB-7 among laterite and Taghma-1 among kaolinite showed higher CEC values. The results in this study revealed that pH values around the neutral range (6.5 to 7.5) resulted in higher values of CEC, as was observed in both laterite and kaolinite samples, except for Taghma-1. Much lower values of Kaolinite CEC were reported by Hisseini et al. [73]; however, laterite CEC values are in line with the results of Ko [67].

The results obtained for the elemental composition of selected laterite and kaolinite samples using XRF are presented in Table 1. The elemental analysis showed that the main constituents of laterite samples are Fe₂O₃, Al₂O₃ and SiO₂, which contributed around 24% to 58%, 5 to 13% and 0.8 to 3%, respectively. Laterites are mostly characterized by the presence of iron and aluminum oxides as major constituents as a product of intense weathering [74]. Similar values of Fe₂O₃ and Al₂O₃ for laterite derived from different geographical regions (India and Vietnam) were reported in the literature, such as Fe₂O₃ (51%) and Al₂O₃ (12.5%) [31], and Fe₂O₃ (49%) and Al₂O₃ (18%) [75]. However, lateritic soils contrarily have lower quantities of Fe₂O₃ [76,77]. The availability of Fe and Al compounds makes laterite a unique material that can act as a potential sorbent for As removal [31,40,78].

Partey [78] also reported Fe₂O₃, Al₂O₃ and SiO₂ as major oxides in the laterites, while CaO, P₂O₅ and K₂O were also present as minor components. The results of this study are in line with outcomes that reported similar values of Fe₂O₃ for raw laterite. On the other hand, elemental analysis of kaolinite samples showed that SiO₂ (6–14%) and Al₂O₃ (5–10%) were the major oxides, as they are part of tetra and octahedral sheets, while other minor oxides are Fe₂O₃, CaO, P₂O₅, K₂O, TiO₂ and Mn₂O₃. These results confirm that this clay is an aluminosilicate material. David et al. [79] reported the presence of SiO₂, Al₂O₃ and Fe₂O₃ in raw kaolin deposits which they related to kaolinite, quartz and hematite as major components. However, in some previous studies, significantly higher values of SiO₂ (47–57%) and Al₂O₃ (22–40%) were reported for raw kaolin, compared to the present study [80–82].

3.2. Arsenic Adsorption by Laterite and Kaolinite

Adsorption isotherms for different laterite and kaolinite samples are shown in Figure 2a,b. A pronounced variation in the As adsorption behavior was observed among laterite samples, whereas kaolinite samples varied nominally, as obvious from the rise of the isotherms below the equilibrium concentration of 20 mg L⁻¹, both for laterite and kaolinite. Generally, laterite isotherms indicated a higher rate of adsorption (up to ~800 mg kg⁻¹) compared to the kaolinite, which achieved adsorbed concentration of ~600 mg kg⁻¹. In Figure 2a, it can be observed that laterite sample HB-7 has not reached the maxima and it can adsorb

more than 1000 mg of As per kg of adsorbent. The remaining laterite samples' isotherms indicated that they can adsorb ~800 mg of As per kg of adsorbent used. In a study, raw laterite collected from India showed notably lower AsV and AsIII adsorption (100 to 120 mg kg⁻¹) [31]. Natural laterite collected from Vietnam also showed slightly lower adsorption of AsV and AsIII (400 to 600 mg kg⁻¹) compared to the present study [75]. However, acid–base treated laterite on the other hand showed much higher adsorption (up to ~4000 mg kg⁻¹) for AsV and AsIII [31,39]. Similarly modified kaolinite also showed higher adsorption of As (2000 to 2500 mg kg⁻¹) compared to materials used in this study [82].

The fast increase in the sorption of As in the case of laterite was observed as sorbed concentration reached ~300 mg kg⁻¹ with a small increase (~3 mg L⁻¹) in the equilibrium concentration. Similar behavior of the As isotherm, as in the fast initial rise and moderate increase in the lateral section of the isotherm, was reported by previous studies [39,75]. A higher rate of adsorption in the laterite in comparison with kaolinite may be correlated with a higher amount of iron and aluminum oxides in laterites. The role of iron and aluminum oxides in laterite for As sorption is already well explained in the literature [31,75].

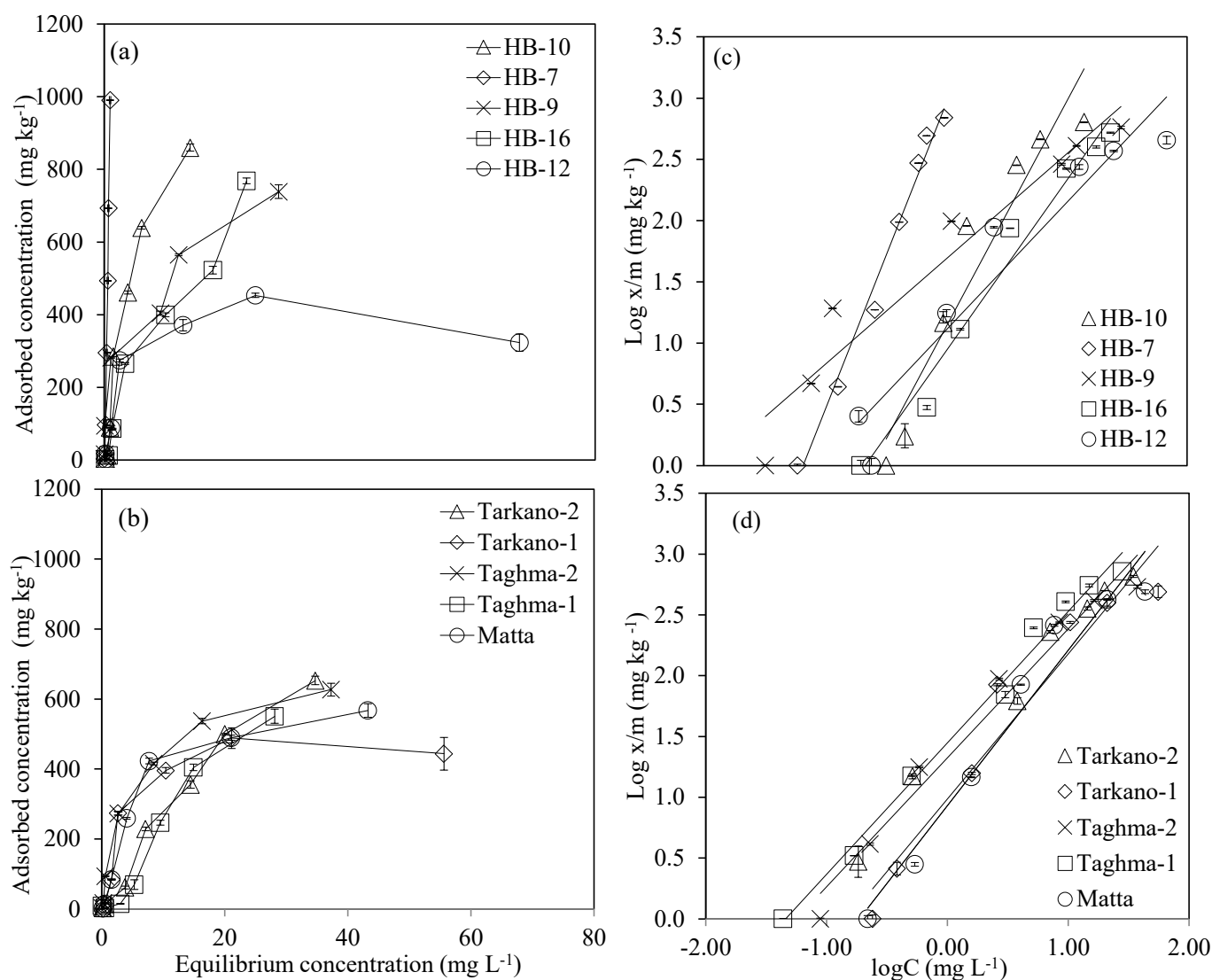


Figure 2. Adsorption isotherms of (a) laterite and (b) kaolinite, (c,d) depicts the Freundlich Equation (4) fit for As in the laterite and kaolinite, respectively. The trend line equation was solved to get adsorption parameters. Error bars indicate the standard deviation among replicates ($n = 3$).

The Langmuir and Freundlich sorption models were then used to explain the sorption isotherms data. The data of the present study fitted well in the Freundlich sorption

model, and the Langmuir model was unable to fit the sorption data both for laterite and kaolinite samples. The Freundlich isotherm can be theoretically derived by assuming that the adsorbent surface is heterogeneous, that is, the adsorption sites are grouped in one patch and distributed exponentially to the adsorption energy. In addition, the adsorption energy usually differs between patches. The Freundlich isotherm gave a better description of the equilibrium behavior, indicating that the sorbents used in this study had a heterogeneous surface, and adsorption energy, which is formed by the interaction between the adsorbate and the adsorbent, was distributed following the exponential decay function. That is why only the results of the Freundlich model parameters are given below.

3.3. Freundlich Model Parameters

Data for As sorption on different laterite and kaolinite types fitted well in the Freundlich equation (Figure 2c,d). The coefficient of regression (R^2) values for laterite were in the range of 0.93 to 0.99, and for kaolinite were in the range of 0.94 to 0.99. The adsorption parameters obtained from the linear regression equation are presented in Table 2. The adsorption intensity, β , was in the range of 0.46 to 1.16 for laterite, and kaolinite was in the range of 0.78 to 0.98, while relative adsorption capacity, k_f , was in the range of 8.52 L kg⁻¹ to 1191 L kg⁻¹, and kaolinite ranged from 9.12 L kg⁻¹ to 28 L kg⁻¹. Overall, it seems that kaolinite had a slightly higher adsorption intensity for As than laterite, except for HB-9, which showed the highest (1.16) adsorption intensity, and laterite had more adsorption capacity compared to kaolinite, with an exceptional high of 1191 L kg⁻¹ for HB-7. In the Freundlich isotherm, the value of β was >1 in most laterite and kaolinite samples, indicating chemical adsorption on the heterogeneous surfaces of the sorbent [83,84]. The applicability of Freundlich isotherm in the present study allowed for predicting that multilayer adsorption took place, which is in line with the results of Sanou et al. [44]. The chemisorption route of As adsorption was also observed for laterite and bentonite derived from India [77].

Table 2. Fitted Freundlich adsorption model parameters for laterite and kaolinite.

Sample	β	k_f L kg ⁻¹	R^2
Laterite			
HB-10	0.74 _(0.29)	13.71 _(2.76)	0.93
HB-7	0.46 _(0.06)	1191 _(272.0)	0.99
HB-9	1.16 _(0.007)	48.10 _(1.83)	0.95
HB-16	0.71 _(0.018)	8.52 _(0.72)	0.98
HB-12	0.97 _(0.09)	12.99 _(3.52)	0.93
Kaolinite			
Tarkano-2	0.98 _(0.10)	22.09 _(7.68)	0.99
Tarkano-1	0.85 _(0.05)	9.84 _(2.07)	0.94
Taghma-2	0.94 _(0.02)	21.13 _(1.86)	0.98
Taghma-1	0.93 _(0.01)	28.04 _(0.66)	0.99
Matta	0.78 _(0.01)	9.12 _(0.47)	0.97

Higher adsorption capacities for laterite are probably due to higher levels of iron and aluminum oxides, as a positive correlation of adsorption capacity, k_f , was observed with Fe₂O₃ (r 0.3) and Al₂O₃ (r 0.4). In this study, the Freundlich model was well fitted to the batch experiment data, which is in agreement with the findings of Maji et al. [40] and Nguyen et al. [83]. Also, Maji et al. [74] used the Freundlich model for laterite soils and found lower values for adsorption capacity and higher adsorption intensity values compared to the present study.

Kaolinite had significantly lower values for Fe_2O_3 , but the adsorption of As in kaolinite might be contributed by Al_2O_3 and TiO_2 . Glocheux et al. [85] also reported the role of Al_2O_3 and TiO_2 in the adsorption of AsIII and AsV. Almost similar values of adsorption capacity and adsorption intensity for kaolinite-supported nanocomposites were observed by fitting the Freundlich adsorption model [49]. Mudzielwana et al. [82] reported an adsorption capacity of 2.3 mg g^{-1} for AsIII, and 2.88 mg g^{-1} for AsV, for surfactant-modified kaolin clay mineral, and found that surfactant-modified kaolin clay showed good adsorption capacity towards As, as compared to unmodified kaolin clay mineral.

Mohapatra et al. [72] compared kaolinite with illite and montmorillonite as adsorbates for As removal. The Freundlich adsorption parameters showed kaolinite is a better adsorber for As than illite and montmorillonite.

Based on the above results, it could be concluded that raw laterite and kaolinite are potential adsorbents for As removal from aqueous solution. The adsorption capacities of both adsorbents are comparable with acid–base-treated laterite, and kaolinite modified with hexadecyl-trimethylammonium bromide (HDTMA-Br) cationic surfactant, in previous studies [31,82].

3.4. Adsorption Kinetics

To find out the efficiency of the As adsorption mechanism, optimum contact time for As uptake as well as the rate-limiting step, two kinetic models, viz., a pseudo-first-order model based on physisorption and a pseudo-second-order reaction model based on chemisorption, were analyzed. The initial concentration of As was fixed at 0.5 mg L^{-1} and the adsorbent dose was 30 g L^{-1} . The shaking time was varied in the range of 0–12 h. It was observed that As removal was rapid within 120 min of contact time and relatively slower at contact beyond 120 min. This rapid removal below 120 min indicates the greater number of available sites for the As on the surface of the adsorbent. However, 4 h contact time was sufficient to get the maximum As adsorption with continuous agitation.

Pseudo-first-order and pseudo-second-order reaction models are expressed in Equations (5) and (6). The nonlinear plot of As adsorbed amount, q_t (mg g^{-1}), versus variable time intervals is shown in Figure 3. The parameters for pseudo-first-order and pseudo-second-order models are presented in Table 3.

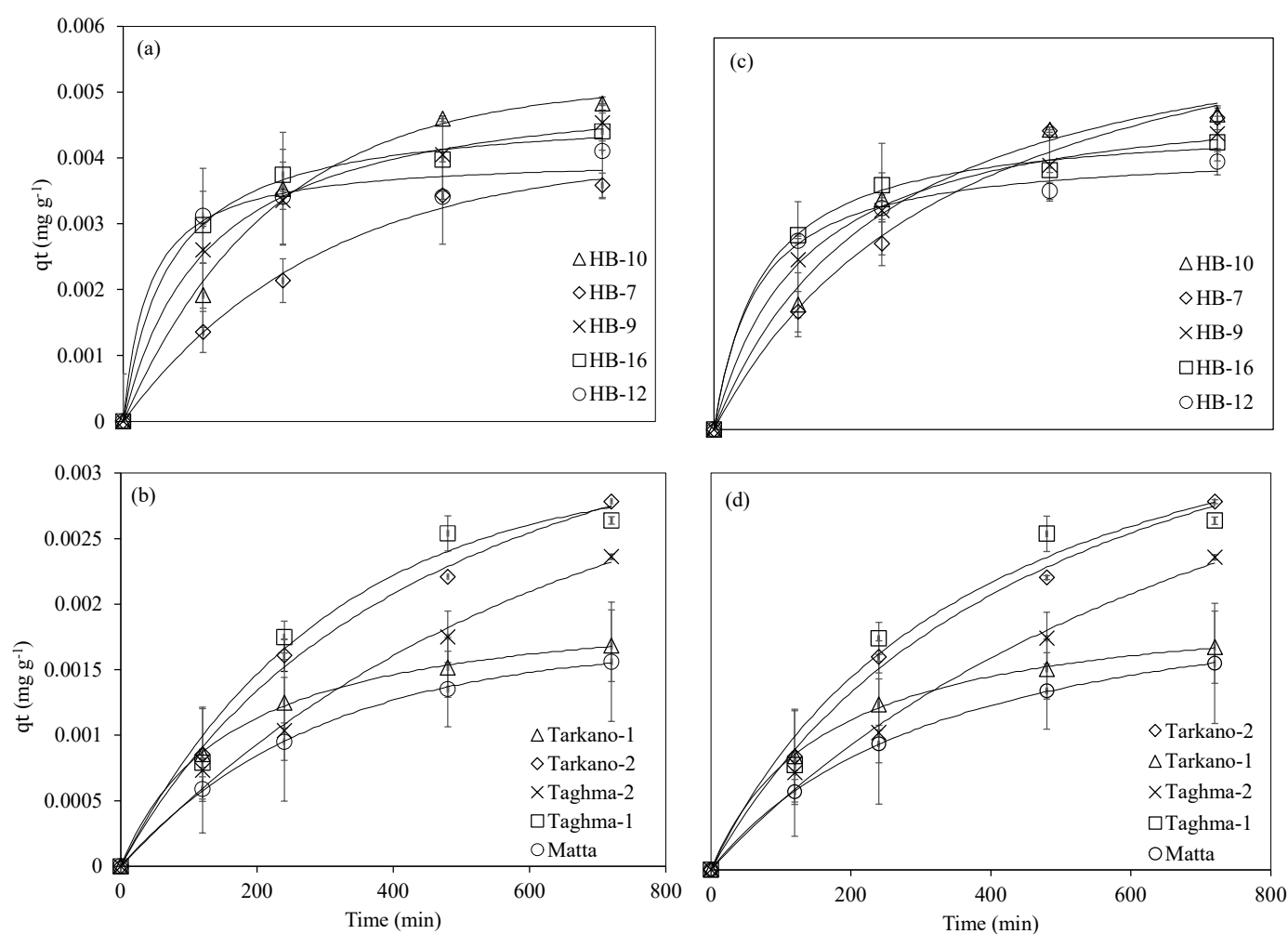


Figure 3. The pseudo-first-order equilibrium model fits for (a) laterite and (b) kaolinite and pseudo-second-order equilibrium model fits for (c) laterite and (d) kaolinite.

Table 3. Pseudo-first-order and pseudo-second-order reaction model parameters.

Samples	Pseudo-First Order			Pseudo-Second Order		
	q_e mg g ⁻¹	k_1 min ⁻¹	R ²	q_e mg g ⁻¹	k_2 g mg ⁻¹ min ⁻¹	R ²
Laterite						
HB10	0.0053(0.0004)	0.0046(0.0023)	0.990	0.0063(0.0012)	0.6218(0.7977)	0.976
HB-7	0.0053(0.0003)	0.0032(0.0001)	0.980	0.0074(0.0005)	0.3749(0.0779)	0.973
HB-9	0.0045(0.0008)	0.0085(0.0046)	0.966	0.0055(0.0017)	2.6543(2.1387)	0.973
HB-16	0.0042(0.0001)	0.0098(0.0012)	0.980	0.0047(0.0002)	3.1406(0.2822)	0.986
HB-12	0.0037(0.0001)	0.0205(0.0167)	0.946	0.0042(0.0002)	3.8895(0.8504)	0.990
Kaolinite						
Tarkano-2	0.0032(0.0002)	0.0027(0.0003)	0.983	0.0046(0.0004)	0.4446(0.1197)	0.990
Tarkano-1	0.0016(0.0002)	0.0058(0.002)	0.986	0.0020(0.0001)	3.0504(1.1881)	0.990
Taghma-2	0.0119(0.010)	0.0043(0.003)	0.983	0.1582(0.24)	1.4279(1.3009)	0.990
Taghma-1	0.0030(0.0001)	0.0033(0.0002)	0.973	0.0042(0.0002)	0.6053(0.0878)	0.966
Matta	0.0017(0.0006)	0.0036(0.0013)	0.990	0.0024(0.001)	1.7209(1.4572)	0.990

In the case of pseudo-first order, the sorbed amount at equilibrium, q_e , for laterite is in the range of 0.0037 to 0.0053 mg g⁻¹, while for kaolinite it is in the range of 0.0016–0.0119

mg g⁻¹. Overall, laterite showed a higher sorbed amount at equilibrium compared to kaolinite, except for Taghma-2. The values of the pseudo-first-order rate constant k_1 for laterite are in the range of 0.0032–0.02 min⁻¹, and for kaolinite are in the range of 0.0027–2.48 min⁻¹. Similarly, the pseudo-second-order rate constant k_2 for laterite is in the range of 0.3749–3.3890 g mg⁻¹ min⁻¹, and for kaolinite is in the range of 0.0027–2.48 min⁻¹. Arsenic adsorption kinetics of clay minerals (nontronite, montmorillonite and kaolinite) showed higher q_e values (0.179 to 0.267 mg g⁻¹) and lower k_1 (0.001 to 0.0032 min⁻¹) and k_2 (0.0191 to 0.066 g mg⁻¹ min⁻¹) values compared to the materials used in this study [86]. In another study, iron oxide-coated rock was used for As adsorption, in which k_2 and q_e were 0.033 g mg⁻¹ min⁻¹ and 4.18 mg g⁻¹, respectively [74]. Arsenic species adsorption (AsV and AsIII) on surfactant-modified kaolinite showed q_e values in the range of 2.1 to 4 mg g⁻¹, and k_1 and k_2 values in the range of 0.09 to 0.1 and 0.03 g mg⁻¹ min⁻¹ to 0.27 g mg⁻¹ min⁻¹, respectively [82].

The pseudo-second-order parameters, viz., q_e and k_2 values, are greater than pseudo-first-order reaction parameters, and k_2 is many folds higher as compared to k_1 . Overall, q_e and k_2 values for laterite are greater than kaolinite values except for Taghma-2 which had exceptionally higher values of q_e , which were similar to the q_e values of pseudo-first-order parameters.

Ghorbanzadeh et al. [86] studied the As adsorption on different clay minerals, and kinetic studies of As forms showed that the sorption mechanism was well explained by a pseudo-second-order model, and the results of pseudo-first-order parameters were in line with the present study. The kinetic behavior of As adsorption on laterite soil in an aqueous medium was studied by Maji et al. [40], employing both pseudo-first-order and pseudo-second-order kinetic models, and found that a pseudo-second-order kinetic model best described the adsorption process. Similarly, Maiti et al. [38] also reported that As adsorption on laterite was well explained by a pseudo-second-order reaction. In another study, laterite was used for the removal of As from groundwater. The kinetic modeling in the study, by considering the pattern of the plots and comparing the q_e values qualitatively, concluded that the pseudo-second-order model better describes the behavior of As adsorption by laterite [87].

In the present study, the correlation coefficients (R^2) for the pseudo-first- and pseudo-second-order equations are satisfactory (Table 3), which means that the sorption follows both equilibrium models fairly well, possibly because total As contains both AsIII and AsV, and in the pH range of 5 to 7 both AsIII and AsV can exist, which results in the sorption following a mixed model [82]. However, the R^2 of the pseudo-second-order equation is better than the pseudo-first order's for most laterite and kaolinite samples, suggesting the chemisorption of As on clay materials as a predominant mechanism [82]. Ho and McKay [88] stated that the adsorption mechanism is mainly chemisorption when it follows the pseudo-second-order kinetic model. According to the pseudo-second-order adsorption rate constant k_2 , it can be concluded that the adsorption process on laterite reached a faster equilibrium than that of kaolinite.

Thus, from the present kinetic reaction study, it may be concluded that the sorption of As on laterite and kaolinite can be better explained by the pseudo-second-order kinetic model than the pseudo-first-order kinetic model.

3.5. FTIR Spectra

FTIR spectra of raw laterite and kaolinite before and after adsorption are depicted in Figures 4 and 5. For laterite, in Figure 4, it was observed that there is a broad stretch at 3200 to 3400 cm⁻¹ with a peak at 3330 cm⁻¹, confirming the presence of the hydroxyl group (bonded-OH stretch) in the post adsorption sample, as the range between 3370–3405 cm⁻¹ is designated for OH stretch [89]. The broad bands around 3330 and 1634 cm⁻¹ in post-adsorption samples were assigned to adsorbed water, as a range of around 3365 and 1635 cm⁻¹ for adsorbed water was also reported by Mbaye et al. [90]. Separately, a range of 1620–1640 cm⁻¹ responsible for interlayer water molecules between the adsorbent layer

was also reported by Saadon et al. [89]. The sharp peaks at 980 and 528 cm^{-1} confirmed the presence of Al-OH and Fe-O bond stretching with slight variation in frequency (912 and 543 cm^{-1}) reported by Saadon et al. [89]. Maiti et al. [31] related the peaks of 535 and 472 cm^{-1} with the presence of hematite in laterite.

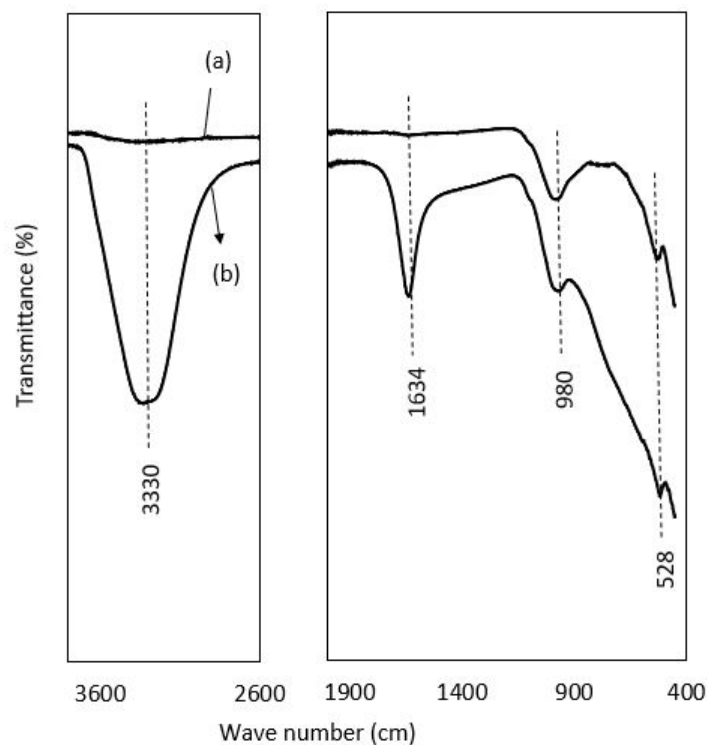


Figure 4. FTIR spectra showing the peak values of transmittance against wave numbers: (a) represents the spectra of raw laterite, and (b) is the spectra of laterite after adsorption.

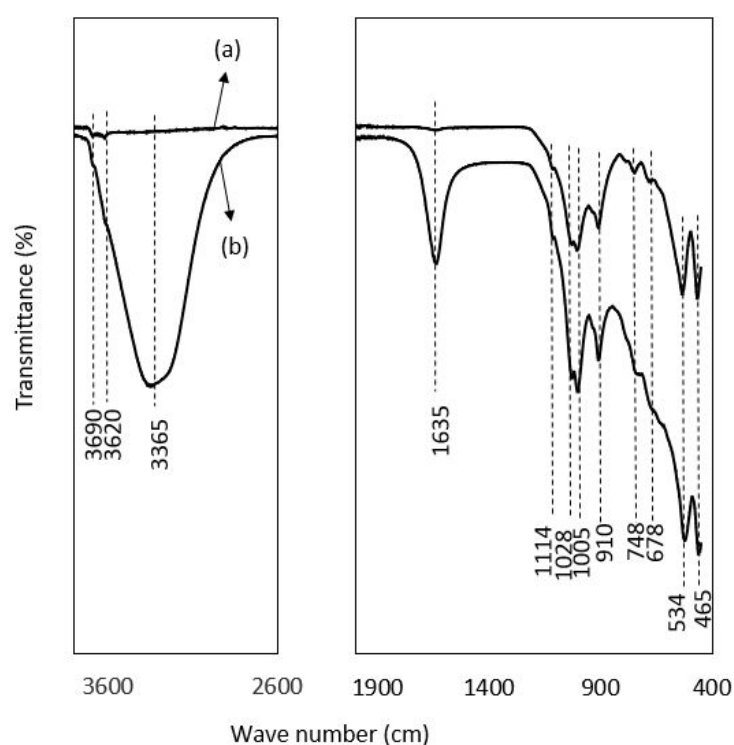


Figure 5. FTIR spectra showing the peak values of transmittance against wave numbers: (a) represents the spectra of raw kaolinite, and (b) is the spectra of laterite after adsorption.

In the FTIR patterns of kaolinite (Figure 5), the bands range between 3620, 3690 and 3665 cm^{-1} in the case of the post-adsorption kaolinite sample, representing the -OH stretching vibration of the adsorbed water molecule, as the range between 3669 and 3696 cm^{-1} is designated for OH stretch [90]. Similarly, the bands located at 3696, 3669 and 3652 cm^{-1} are the typical signature of the inner-surface hydroxyls of kaolinite, and the peak at 3619 cm^{-1} is attributed to the stretching frequency of the internal hydroxyl groups [91]. The broad bands around 3365 and 1635 cm^{-1} are due to the adsorbed water in post-adsorption sample of kaolinite. The bands with a slight variation at 1028, 910, 1005 and 748 cm^{-1} represent the vibration of Si-O-Fe, Si-O, Al-OH, and Fe-OH, respectively, as the values of 1034, 1008, 911, and 795 cm^{-1} assigned to these groups [31]. Ioannou et al. [92] also reported almost similar band values frequency for kaolinite-hematite composite. The peak value at 910 is attributed to the Al-OH bond stretching, as Maiti et al. [39] reported 912 cm^{-1} for this group. Moreover, the bands at 534 and 465 cm^{-1} in kaolinite can be ascribed to the vibration of Si-O-Al/Fe, Si-O-Si and Al-O, as the range of 573 and 473 cm^{-1} has been studied in previous studies [93]. The specific peak at 534 is attributed to the Al-O bending vibration [94]. The peaks at 748 and 465 are related to the presence of quartz as Mustapha et al. [95] attributed 750 and 467 cm^{-1} to quartz. The band at 1114 cm^{-1} corresponds to the stretching vibrations of the Si-O-Si group, as described by Mbaye et al. [90] in the range of 1100 cm^{-1} . Jalees et al. [50] reported almost similar bands with slight variation in the frequency for a local kaolin called chikini mitti, obtained from the market. All the peaks in laterite and kaolinite were more intensified after adsorption.

3.6. Degree of Lateritization

Laterite composition widely varies with extent of lateritization, parent rock and geographical location [96]. Lateritization by hydrolysis and oxidation removes silica from the parent rock, leading to the formation of laterite concretion or laterite soil. The degree of lateritization is defined as the silica-sesquioxide (S-S) ratio. The degree of lateritization is estimated by using the expression: $(\text{SiO}_2/(\text{Fe}_2\text{O}_3 + \text{Al}_2\text{O}_3))$. The ratios for all raw laterite samples used in this study were calculated from chemical composition data obtained from XRF results. The values of S-S for laterite used in the present study were in the range of 0.04, 0.06, 0.04, 0.047 and 0.015. According to Partey [78], all laterite samples with S-S values below 1.33 are characterized as laterite. All collected samples are classified as laterite or laterite concretion according to categories developed based on the degree of lateritization [31]. The information on As removal efficiency compared with different laterite compositions collected from different geographical locations is scarce. In this study laterite samples collected from different locations showed a high degree of lateritization which means they have a higher percentage of iron and aluminum oxides compared to the raw laterite used for As removal by Maiti et al. [31]. The iron and aluminum oxide percentage in laterite is important for its As removal efficiency.

3.7. SEM-EDX

The morphology of selected laterite and kaolinite samples before and after sorption are shown in Figure 6a–d, along with the EDX spectra in Figure 6e–h. The SEM images revealed that the surfaces of the laterite and kaolinite are rough, along with particles having irregular shapes and sizes. The presence of a large number of such particles may attribute to the nanostructures and magnetic properties [97], which contribute to the tendency for agglomeration and aggregation. The SEM images of laterite and kaolinite before and after sorption reveal clear changes in the morphology, which can be attributed to the adsorption of As in the pores and the roughness of the natural laterite and kaolinite surface. It can be seen that laterite and kaolinite have sheet-like morphology, which indicates the layered structure of the sorbents. The EDX spectrum of the laterite before and after sorption shows peaks of Fe and Al, which confirms the presence of Fe and Al oxides as a major constituent. Similarly, the EDX spectrum of kaolinite before and after sorption shows the peaks of Al and Si as major constituents, while Fe is in much lesser quantities.

The EDX results of laterite and kaolinite are in line with the data of XRF. Hence, the role of Fe and Al oxides in the case of laterite, and Al oxides in the case of kaolinite, is clear. Based on the results, it is very much evident that the surface complexation reaction has occurred between aqueous As and sorbents (laterite and kaolinite). Thus, the sorbents used in this study have proven to be one of the most efficient sorbents for aqueous As remediation.

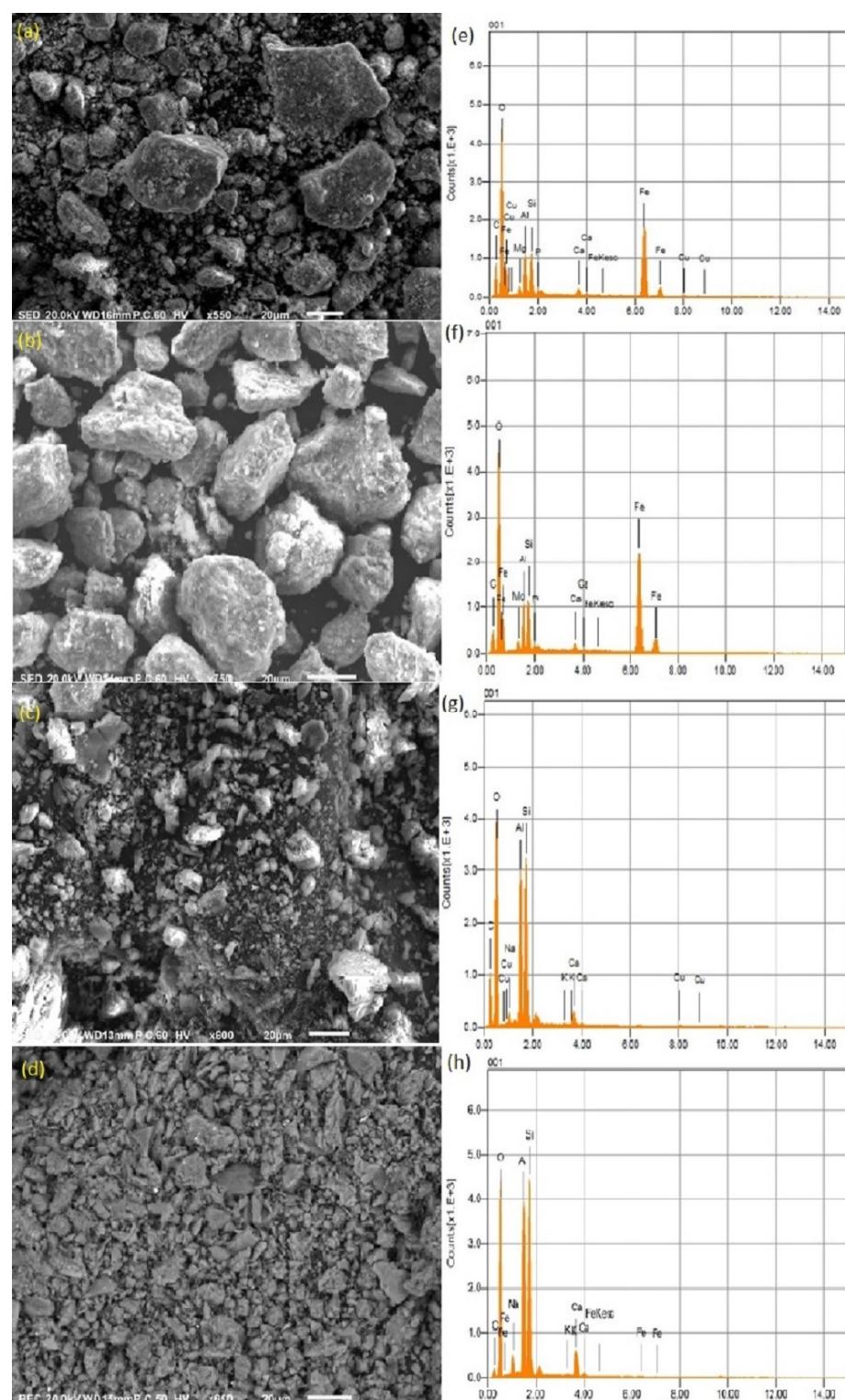


Figure 6. SEM micrographs along with EDX plots of a selected laterite (a,b,e,f) and kaolinite (c,d,g,h) samples taken before and after sorption.

4. Conclusions

In the present study, indigenous deposits of laterite and kaolinite were studied for their adsorption potential for As, and for understanding the mechanism of As adsorption. The morphological and structural analysis (FTIR and SEM-EDX) are in agreement with the XRF analysis, and confirm the role of Fe and Al oxides in As sorption onto laterite and kaolinite. Among Langmuir and Freundlich sorption models, the Freundlich isotherm model well explained the sorption of As on the heterogeneous surfaces of the sorbents. The sorption parameters indicated that laterite had greater adsorption capacity than kaolinite, while both showed almost similar intensities for As. Also, a pseudo-second-order equation better fitted the experimental data, suggesting that both physical and chemical sorption contributed to the overall sorption of As onto laterite and kaolinite, but chemical sorption contributed more, especially in the case of kaolinite. Experimental results demonstrated that naturally occurring laterite and kaolinite are quite effective sorbents for the removal of As from an aqueous solution. It has also been observed that laterite exhibited the maximum removal of As and thus proved to be superior in comparison with kaolinite. Thus, these naturally existing substances may have some applied significance as sorbent agents at the domestic level to provide safe consumable water.

Author Contributions: S.R. conceived the idea. A.R. and H.S. conducted the experiment. K.M.M. and L.A. carried out the literature review. A.M. and A.K. provided technical expertise to strengthen the basic idea. A.Q. and S.A.K. helped with the statistical analysis. S.A.A. proofread and provided intellectual guidance. All authors read the first draft, helped in revision, and approved the article. All authors have read and agreed to the published version of the manuscript.

Funding: The authors would like to acknowledge the support of Prince Sultan University for paying the article processing charges of this publication.

Institutional Review Board Statement: Not applicable.

Informed Consent Statement: Not applicable.

Data Availability Statement: The data presented in this study are available on request from the corresponding author.

Acknowledgments: The authors would like to thank the support of Prince Sultan University for paying the article processing charges of this publication.

Conflicts of Interest: The authors declare no conflict of interest.

References

1. Mazumder, G. Chronic arsenic toxicity & human health. *Indian J. Med. Res.* **2008**, *128*, 436–447.
2. Mandal, B.K.; Suzuki, K.T. Arsenic round the world: A review. *Talanta* **2002**, *58*, 201–235. [https://doi.org/10.1016/S0039-9140\(02\)00268-0](https://doi.org/10.1016/S0039-9140(02)00268-0).
3. Jain, C.K.; Ali, I. Arsenic: Occurrence, toxicity and speciation techniques. *Water Res.* **2000**, *34*, 4304–4312. [https://doi.org/10.1016/S0043-1354\(00\)00182-2](https://doi.org/10.1016/S0043-1354(00)00182-2).
4. Mudhoo, A.; Sharma, S.K.; Garg, V.K.; Tseng, C.H. Arsenic: An overview of applications, health, and environmental concerns and removal processes. *Crit. Rev. Environ. Sci. Technol.* **2011**, *41*, 435–519.
5. Kitchin, K.T. Recent advances in arsenic carcinogenesis: Modes of action, animal model systems, and methylated arsenic metabolites. *Toxicol. Appl. Pharmacol.* **2001**, *172*, 249–261. <https://doi.org/10.1006/taap.2001.9157>.
6. Maiti, A.; DasGupta, S.; Basu, J.K.; De, S. Adsorption of arsenite using natural laterite as adsorbent. *Sep. Purif. Technol.* **2007**, *55*, 350–359. <https://doi.org/10.1016/j.seppur.2007.01.003>.
7. Wang, S.; Mulligan, C.N. Occurrence of arsenic contamination in Canada: Sources, behavior and distribution. *Sci. Total Environ.* **2006**, *366*, 701–721. <https://doi.org/10.1016/j.scitotenv.2005.09.005>.
8. Nishimura, T.; Robins, R.G. A re-evaluation of the solubility and stability regions of calcium arsenites and calcium arsenates in aqueous solution at 25 °C. *Miner. Process. Extr. Metall. Rev.* **1998**, *18*, 283–308. <https://doi.org/10.1080/08827509808914159>.
9. Bothe, J.V.; Brown, P.W. Arsenic immobilization by calcium arsenate formation. *Environ Sci Technol* **1999**, *33*, 3806–3811.
10. Cullen, W.R.; Reimer, J.K. Arsenic speciation in the environment. *Chem. Rev.* **1989**, *4*, 713–764. <https://doi.org/10.1021/cr00094a002>.
11. Shankar, S.; Shanker, U.; Shikha. Arsenic Contamination of Groundwater: A Review of Sources, Prevalence, Health Risks, and Strategies for Mitigation. *Sci. World J.* **2014**, *2014*, 18. <https://doi.org/10.1155/2014/304524>.

12. McCarty, K.; Hanh, H.; Kim, K. Arsenic geochemistry and human health in South East Asia. *Rev. Environ. Health* **2011**, *26*, 71–78. <https://doi.org/10.1515/reveh.2011.010>.
13. Jessen, S. Groundwater Arsenic in the Red River Delta, Vietnam: Regional Distribution, Release, Mobility and Mitigation Options. Technical University of Denmark. 2009. Available online: <http://www.er.dtu.dk/publications/fulltext/2009/ENV2009-208.pdf> (accessed on 13 March 2022).
14. Podgorski, J.E.; Eqani, S.A.M.A.S.; Khanam, T.; Ullah, R.; Shen, H.; Berg, M. Extensive arsenic contamination in high-pH unconfined aquifers in the Indus Valley. *Sci. Adv.* **2017**, *3*, e1700935. <https://doi.org/10.1126/sciadv.1700935>.
15. Nickson, R.T.; McArthur, J.M.; Sherestha, B.; Kyaw-Myint Lowry, D. Arsenic and other drinking water quality issues, Muzaffargarh District, Pakistan. *Appl. Geochem.* **2005**, *20*, 55–68. <https://doi.org/10.1016/j.apgeochem.2004.06.004>.
16. Pak-EPA, Pakistan Environmental Protection Agency. *Ministry of Environment, National Standards for Drinking Water Quality (NSDWQ)*; Pak-EPA, Pakistan Environmental Protection Agency: Islamabad, Pakistan, 2008.
17. Elizade-González, M.P.; Mattusch, J.; Einicke, W.D.; Wennrich, R. Sorption on natural solids for arsenic removal. *Chem. Eng. J.* **2001**, *81*, 187–195. [https://doi.org/10.1016/S1385-8947\(00\)00201-1](https://doi.org/10.1016/S1385-8947(00)00201-1).
18. World Health Organization (WHO). *Guidelines for Drinking-Water Quality*, 3rd ed.; WHO: Geneva, Switzerland, 2004; Volume 1.
19. Hughes, M. Arsenic toxicity and potential mechanisms of action. *Toxicol. Lett.* **2002**, *133*, 1–16. [https://doi.org/10.1016/S0378-4274\(02\)00084-X](https://doi.org/10.1016/S0378-4274(02)00084-X).
20. Steinmaus, C.; Yaun, Y.; Bates, M.N.; Smith, A.H. Case-control study of bladder cancer and Drinking Water Arsenic in the Western United States. *Am. J. Epidemiol.* **2003**, *158*, 1193–1201. <https://doi.org/10.1093/aje/kwg281>.
21. Sampson, M.; Bostick, B.; Chiew, H.; Hagan, J.; Shantz, A. Arsenicosis in Cambodia: Case studies and policy response. *Appl. Geochem.* **2008**, *23*, 2977–2986. <https://doi.org/10.1016/j.apgeochem.2008.06.022>.
22. Yuan, C.; Chiang, T.-S. The mechanisms of arsenic removal from soil by electrokinetic process coupled with iron permeable reaction barrier. *Chemosphere* **2007**, *67*, 1533–1542. <https://doi.org/10.1016/j.chemosphere.2006.12.008>.
23. Shen, Y.S. Study of Arsenic Removal from Drinking Water. *J. Am. Water Works Assoc.* **1973**, *65*, 543–548. <https://doi.org/10.1002/j.1551-8833.1973.tb01892.x>.
24. Sorg, T.J.; Logsdon, G.S. Treatment technology to meet the interim primary drinking water regulations for inorganics: Part 2. *J. Am. Water Works Assoc.* **1978**, *70*, 379–393. <https://doi.org/10.1002/j.1551-8833.1978.tb04198.x>.
25. Hisa, T.H.; Lo, S.L.; Lin, C.F.; Lee, D.Y. Characterization of arsenate adsorption on hydrous iron oxide using chemical and physical methods. *Colloids Surf. A Physicochem. Eng. Asp.* **1994**, *85*, 1–7. [https://doi.org/10.1016/0927-7757\(94\)02752-8](https://doi.org/10.1016/0927-7757(94)02752-8).
26. Cheng, C.; Kacherovsky, N.; Dombek, K.M.; Camier, S.; Thukral, S.K.; Rhim, E.; Young, E.T. Identification of potential target genes for Adr1p through characterization of essential nucleotides in UAS1. *Mol. Cell Biol.* **1994**, *14*, 3842–3852. <https://doi.org/10.1128/mcb.14.6.3842-3852.1994>.
27. Scott, K.N.; Green, J.F.; Do, H.D.; Mclean, S.J. Arsenic Removal by Coagulation. *J. Am. Water Works Assoc.* **1995**, *87*, 114–126. <https://doi.org/10.1002/j.1551-8833.1995.tb06347.x>.
28. McNeill, L.S.; Edwards, M. Soluble arsenic removal at water treatment plants. *J. Am. Water Works Assoc.* **1995**, *87*, 105–187. <https://doi.org/10.1002/j.1551-8833.1995.tb06346.x>.
29. Fox, K.R.; Sorg, T.J. Controlling Arsenic, Fluoride, and Uranium by Point-of-Use Treatment. *J. Am. Water Works Assoc.* **1987**, *79*, 81–84. <https://doi.org/10.1002/j.1551-8833.1987.tb02928.x>.
30. Kumar, A.; Singh, K.; Dixit, U.; Bhat, R.A.; Gupta, S.P. Removal of Arsenic—“A Silent Killer” in the Environment by Adsorption Methods. In *Arsenic Monitoring, Removal and Remediation*; Stoytcheva, M., Zlatev, R., Eds.; IntechOpen: London, UK, 2021. <https://doi.org/10.5772/intechopen.98985>.
31. Maiti, A.; Thakur, B.K.; Basu, J.K.; De, S. Comparison of treated laterite as arsenic adsorbent from different locations and performance of best filter under field conditions. *J. Hazard. Mater.* **2013**, *262*, 1176–1186. <https://doi.org/10.1016/j.jhazmat.2012.06.036>.
32. Maqsood, H.R.; Rukh, S.; Imran, M.; Mehmood, A.; Ahmad, W.; Matloob, A.; Ahmad, H.S.; Khan, A.; Butt, S.A. Evaluation of laterite as a filter media to remove arsenic from groundwater. *J. Serb. Chem. Soc.* **2021**, *86*, 195–207. <https://doi.org/10.2298/JSC200310057M>.
33. Bentahar, Y.; Hurel, C.; Draoui, K.; Khairoun, S.; Marmier, N. Adsorptive properties of Moroccan clays for the removal of arsenic(V) from aqueous solution. *Appl. Clay Sci.* **2016**, *119*, 385–392. <https://doi.org/10.1016/j.clay.2015.11.008>.
34. Ullah, H.; Nafees, M.; Iqbal, F.; Awan, S.; Shah, A.; Waseem, A. Adsorption Kinetics of Malachite green and Methylene blue from aqueous solutions using surfactant-modified Organoclays. *Acta Chim. Slov.* **2017**, *64*, 449–460. <https://doi.org/10.17344/acsi.2017.3285>.
35. Nafees, M.; Waseem, A. Organoclays as sorbent material for phenolic compounds: A review. *CLEAN—Soil Air Water* **2014**, *42*, 1500–1508. <https://doi.org/10.1002/clen.201300312>.
36. Rizzi, V.; Gubitosa, J.; Fini, P.; Romita, R.; Agostiano, A.; Nuzzo, S.; Cosma, P. Commercial bentonite clay as low-cost and recyclable “natural” adsorbent for the Carbendazim removal/recover from water: Overview on the adsorption process and preliminary photodegradation considerations. *Colloids Surf. A Physicochem. Eng. Asp.* **2020**, *602*, 125060. <https://doi.org/10.1016/j.colsurfa.2020.125060>.
37. Schellmann, W. A new definition of laterite. In *Lateritisation Processes*; IGCP-127; Memoirs of the Geological Survey of India: Calcutta, India, 1986; Volume 120, pp. 1–7.

38. Maiti, A.; DasGupta, S.; Basu, J.K.; De, S. Batch and column study: Adsorption of arsenate using untreated laterite as adsorbent. *Ind. Eng. Chem.* **2008**, *47*, 1620–1629. <https://doi.org/10.1021/ie070908z>.
39. Maiti, A.; Basu, J.K.; De, S. Development of a treated laterite for arsenic adsorption: Effects of treatment parameters. *Ind. Eng. Chem.* **2010**, *49*, 4873–4886. <https://doi.org/10.1021/ie100612u>.
40. Maji, S.K.; Pal, A.; Pal, T. Arsenic removal from aqueous solutions by adsorption on laterite soil. *J. Environ. Sci. Health-Toxic/Hazard.* **2007**, *42*, 453–462. <https://doi.org/10.1080/10934520601187658>.
41. Kundu, S.; Pal, A.; Mandal, M.; Ghosh, S.; Panigrahi, S.; Pal, T. Hardened paste of Portland cement—A new low-cost adsorbent for the removal of arsenic from water. *J. Environ. Sci. Health A Tox Hazard. Subst. Environ. Eng.* **2004**, *39*, 185–202. <https://doi.org/10.1081/ESE-120027377>.
42. Zhang, W.; Singh, P.; Paling, E.; Delides, S. Arsenic removal from contaminated water by natural iron ores. *Miner. Eng.* **2004**, *17*, 517–524. <https://doi.org/10.1016/j.mineng.2003.11.020>.
43. Vaughan, R.L.; Reed, B.E. Modeling As(V) removal by a iron oxide impregnated activated carbon using the surface complexation approach. *Water Res.* **2005**, *39*, 1005–1014. <https://doi.org/10.1016/j.watres.2004.12.034>.
44. Sanou, Y.; Pare SPuong, N.T.T.; Phuoc, N.V. Experimental and kinetic modeling of as (v) adsorption on granular ferric hydroxide and laterite. *J. Environ. Treat. Tech.* **2016**, *4*, 62–70.
45. Tuzen, M.; Melek, E.; Soylak, M. Celtek clay as sorbent for separation–preconcentration of metal ions from environmental samples. *J. Hazard. Mater.* **2006**, *136*, 597–603. <https://doi.org/10.1016/j.jhazmat.2005.12.036>.
46. Chandrasekhar, S.; Ramaswamy, S. Influence of mineral impurities on the properties of kaolin and its thermally treated products. *Appl. Clay Sci.* **2002**, *21*, 133–142. [https://doi.org/10.1016/S0169-1317\(01\)00083-7](https://doi.org/10.1016/S0169-1317(01)00083-7).
47. Hubadillah, S.K.; Othman, M.H.D.; Ismail, A.F.; Rahman, M.A.; Jaafar, J. A low cost hydrophobic kaolin hollow fiber membrane (h-KHFM) for arsenic removal from aqueous solution via direct contact membrane distillation. *Sep. Purif. Technol.* **2019**, *214*, 31–39. <https://doi.org/10.1016/j.seppur.2018.04.025>.
48. Hedfi, I.; Hamdi, N.; Rodriguez, M.A.; Srasra, E. Development of a low cost microporous ceramic membrane from kaolin and Alumina, using the lignite as porosity agent. *Ceram. Int.* **2016**, *42*, 5089–5093. <https://doi.org/10.1016/j.ceramint.2015.12.023>.
49. Ahmad, H.B.; Azhar, M.; Hussain, M.; Shafiq, Z.; Hussain, I.; Arain, S.A. Synthesis and characterization of kaolin supported metallic nanocomposites for the removal of arsenic. *Fresenius. Environ. Bull.* **2015**, *24*, 4019–4024.
50. Jalees, M.I.; Farooq, M.U.; Basheer, S.; Asghar, S. Removal of heavy metals from drinking water using chikni mitti (kaolinite): Isotherm and kinetics. *Arab. J. Sci. Eng.* **2019**, *44*, 6351–6359. <https://doi.org/10.1007/s13369-019-03722-z>.
51. Malkani, M.S.; Khosa, M.H.; Alyani, M.I.; Khan, K.; Somro, N.; Zafar, T.; Arif, J.; Zahid, M.A. Mineral deposits of Khyber Pakhtunkhwa and FATA (Pakistan). *Lasbela U. J. Sci. Tech.* **2017**, *4*, 23–46.
52. Siddiqui, M.A.; Ahmed, Z.; Saleemi, A.A. Evaluation of Swat kaolin deposits of Pakistan for industrial uses. *Appl. Clay Sci.* **2005**, *29*, 55–72. <https://doi.org/10.1016/j.clay.2004.09.005>.
53. Malkani, M.S.; Qazi, S.; Khosa, M.H.; Shah, M.R.; Zafar, T.; Arif, J. Iron, laterite, bauxite and ochre deposits of Pakistan: Emphasis on feasible Dilband and low grade Fort Munro ironstones. In Proceedings of the 5th International Conference on Earth Sciences Pakistan, Baragali Campus, Pakistan, 11–13 August 2018; pp. 11–13.
54. Qasim, M.; Khan, M.A.; Haneef, M. Stratigraphic characterization of the Early Cambrian Abbottabad Formation in the Sherwan area, Hazara region, N. Pakistan: Implications for Early Paleozoic stratigraphic correlation in NW Himalayas, Pakistan. *J. Himal. Earth Sci.* **2014**, *47*, 25–40.
55. Mclean, E.O. Soil pH and lime requirement. In *Methods of Soil Analysis, Part II, Chemical and Microbiological Properties*; Page, A.L., Ed.; American Society of Agronomy: Madison, WI, USA, 1983; p. 199. <https://doi.org/10.2134/agronmonogr9.2.2ed.c12>.
56. Rhoades, J.D. Soluble salts. In *Methods of Soil Analysis, Part II*; Page, A.L., Ed.; American Society of Agronomy: Madison, WI, USA, 1983; pp. 172–173. <https://doi.org/10.2134/agronmonogr9.2.2ed.c10>.
57. Chapmen, H.D. Cation-Exchange Capacity. In *Methods of Soil Analysis. Part 2, Chemical and Microbiological Properties*; Norman, A.G., Ed.; American Society of Agronomy: Madison, WI, USA, 1965; p. 891. <https://doi.org/10.2134/agronmonogr9.2.c6>.
58. Langmuir, I. The adsorption of gases on plane surfaces of glass, mica and platinum. *J. Am. Chem. Soc.* **1918**, *40*, 1361–1403. <https://doi.org/10.1021/ja02242a004>.
59. Syers, J.; Browman, M.; Smillie, G.; Corey, R. Phosphate sorption by soils evaluated by the Langmuir adsorption equation. *Soil Sci. Soc. Am. J.* **1973**, *37*, 358–363. <https://doi.org/10.2136/sssaj1973.03615995003700030015x>.
60. Castro, C.; Rolston, D. Organic phosphate transport and hydrolysis in soil: Theoretical and experimental evaluation. *Soil Sci. Soc. Am. J.* **1977**, *41*, 1085–1092. <https://doi.org/10.2136/sssaj1977.03615995004100060014x>.
61. Freundlich, H. Kapillarchemie. In *Eine Darstellung der Chemie der Kolloide und Verwandter Gebiete*; Akademische Verlagsgesellschaft: Leipzig, Germany, 1909; Volume 15, pp. 948–948.
62. Mendoza-Castillo, D.I.; Rojas-Mayorga, C.K.; Garcia-Martinez, I.P.; Perez-Cruz, M.A.; Hernandez-Montoya, V.; Bonilla-Petriciolet, A.; Montes-Moran, M.A. Removal of heavy metals and arsenic from aqueous solution using textile wastes from denim industry. *Int. J. Environ. Sci. Technol.* **2015**, *12*, 1657–16. <https://doi.org/10.1007/s13762-014-0553-8>.
63. Lee, C.G.; Alvarez, P.J.J.; Nam, A.; Park, S.J.; Do, T.; Choi, U.S.; Lee, S.H. Arsenic(V) removal using an amine-doped acrylic ion exchange fiber: Kinetic, equilibrium, and regeneration studies. *J. Hazard. Mater.* **2017**, *325*, 223–229. <https://doi.org/10.1016/j.jhazmat.2016.12.003>.
64. Zviagina, B.B.; Mccarty, D.K.; Rodon, J.; Drits, V.A. Interpretation of infrared spectra of dioctahedral smectites in the region of OH-stretching vibrations. *Clays Clay Miner.* **2004**, *52*, 399–410. <https://doi.org/10.1346/CCMN.2004.0520401>.

65. Welsh, E.P.; Crook, J.G.; Sanzolone, R. Trace-level determination of arsenic and selenium using continuous-flow hydride generation atomic absorption spectrophotometry (HG-AAS). In *Quality Assurance Manual for the Branch of Geochemistry*; Arbogast, B.F., Eds.; U.S. Geol. Survey: Denver, CO, USA, 1990; pp. 38–45.
66. Moreda-Pineiro, C.; Moscoso-Perez, P.; Lopez-Mahia, S.; Muniategui-Lorenzo, E.; Fernandez-Fernandez Rodriguez, D.P. Multivariate optimisation of hydride generation procedures for single element determinations of As, Cd, Sb, and Se in natural waters by electrothermal atomic absorption spectrometry. *Talanta* **2001**, *53*, 871–883.
67. Ko, T.-H. Nature and properties of lateritic soils derived from different parent materials in Taiwan. *Sci. World J.* **2014**, *2014*, 247194. <https://doi.org/10.1155/2014/247194>.
68. Li, J.; Xu, R. Inhibition of acidification of kaolinite and an Alfisol by aluminum oxides through electrical double-layer interaction and coating. *Eur. J. Soil Sci.* **2013**, *64*, 110–120. <https://doi.org/10.1111/ejss.12021>.
69. Singh, T.S.; Pant, K.K. Equilibrium, kinetics and thermodynamic studies for adsorption of As(III) on activated alumina. *Sep. Purif. Technol.* **2004**, *36*, 139–147. [https://doi.org/10.1016/S1383-5866\(03\)00209-0](https://doi.org/10.1016/S1383-5866(03)00209-0).
70. Gupta, V.K.; Saini, V.K.; Jain, N. Adsorption of As(III) from aqueous solutions by iron oxide-coated sand. *J. Colloid. Interface Sci.* **2005**, *288*, 55–60. <https://doi.org/10.1016/j.jcis.2005.02.054>.
71. Stumm, W. *Chemistry of the Solid-Water Interface: Processes at the Mineral-Water and Particle-Water Interface in Natural Systems*; John Wiley & Son Inc.: Hoboken, NJ, USA, 1992.
72. Mohapatra, D.; Mishra, D.; Chaudhury, G.R.; Das, R.P. Arsenic adsorption mechanism on clay minerals and its dependence on temperature. *Korean J. Chem. Eng.* **2007**, *24*, 426–430. <https://doi.org/10.1007/s11814-007-0073-z>.
73. Hisseini, B.H.A.; Bennabi, A.; Hamzaoui, R.; Makki, L.; Blanck, G. Treatment and recovery of clay soils using geopolymerization method. *Int. J. Geomech.* **2021**, *21*, 04021206. [https://doi.org/10.1061/\(ASCE\)GM.1943-5622.0002150](https://doi.org/10.1061/(ASCE)GM.1943-5622.0002150).
74. Maji, S.; Kao, Y.H.; Liu, C.-W. Arsenic removal from real arsenic-bearing ground water by adsorption on iron-oxide-coated natural rock (IOCNR). *Desalination* **2011**, *280*, 72–79. <https://doi.org/10.1016/j.desal.2011.06.048>.
75. Nguyen, T.H.; Tran, H.N.; Vu, H.A.; Trinh, M.V.; Nguyen, T.V.; Loganathan, P.; Vigneswaran, S.; Nguyen, T.M.; Trinh, V.T.; Vu, D.L.; et al. Laterite as a low-cost adsorbent in a sustainable decentralized filtration system to remove arsenic from groundwater in Vietnam. *Sci. Total Environ.* **2020**, *699*, 134267. <https://doi.org/10.1016/j.scitotenv.2019.134267>.
76. Obianyo, I.I.; Azikiwe, P.O.; Alfred, B.O.; Soboyejo. Mechanical behaviour of lateritic soil stabilized with bone ash and hydrated lime for sustainable building applications. *Case Stud. Constr. Mater.* **2020**, *12*, e00331. <https://doi.org/10.1016/j.cscm.2020.e00331>.
77. Mitra, A.; Mukhopadhyay, P.; Mitra, A. Studies on Removal of Arsenic from Water by Adsorption on Laterite and Ferric-Hydroxide Coated Bentonite. 2014. Available online: <https://ewh.ieee.org/sb/kharagpur/iit/TechSym2014/doc/Paper%20508.pdf> (accessed on 2 April 2022).
78. Partey, F. Mechanism of Arsenic Sorption onto Laterite Concretions. Ph.D. Dissertation, New Mexico Tech University: Socorro, NM, USA, 2008.
79. David, M.K.; Okoro, U.C.; Akpomie, K.G.; Okey, C.; Oluwasola, H.O. Thermal and hydrothermal alkaline modification of kaolin for the adsorptive removal of lead(II) ions from aqueous solution. *SN Appl. Sci.* **2020**, *2*, 1134. <https://doi.org/10.1007/s42452-020-2621-7>.
80. Darban, K.A.; Kianinia, Y.; Taheri-Nassaj, E. Synthesis of nano- alumina powder from impure kaolin and its application for arsenite removal from aqueous solutions. *J. Environ. Health Sci. Eng.* **2013**, *11*, 19. Available online: <http://www.ijehse.com/content/11/1/19> (accessed on 2 April 2022).
81. Marino, T.; Russo, F.; Rezzouk, L.; Bouzid, A.; Figoli, A. PES-Kaolin mixed matrix membranes for arsenic removal from water. *Membranes* **2017**, *7*, 57. <https://doi.org/10.3390/membranes7040057>.
82. Mudzielwana, R.; Gitari, W.; Ndungu, P. Performance evaluation of surfactant modified kaolin clay in As(III) and As(V) adsorption from groundwater: Adsorption kinetics, isotherms and thermodynamics. *Heliyon* **2019**, *5*, e02756. <https://doi.org/10.1016/j.heliyon.2019.e02756>.
83. Nguyen, P.T.N.; Abella, L.C.; Gaspillo, P.D.; Hinode, H. Removal of arsenic from simulated groundwater using calcined laterite as the adsorbent. *J. Chem. Eng. Japan* **2011**, *44*, 411–419. <https://doi.org/10.1252/jcej.11we025>.
84. Bibi, S.; Farooqi, A.; Hussain, K.; Haider, N. Evaluation of industrial based adsorbents for simultaneous removal of arsenic and fluoride from drinking water. *J. Clean Prod.* **2015**, *87*, 882–896. <https://doi.org/10.1016/j.jclepro.2014.09.030>.
85. Glocheux, Y.; Albadarin, A.B.; Galán, J.; Oyedoh, E.; Mangwandi, C.; Gerente, C.; Allen, S.J.; Waker, G.M. Adsorption study using optimised 3d organised mesoporous silica coated with Fe and Al oxides for specific As(III) and As(V) removal from contaminated synthetic groundwater. *Micropor. Mesopor. Mat.* **2014**, *198*, 101–114. <https://doi.org/10.1016/j.micromeso.2014.07.020>.
86. Ghorbanzadeh, N.; Jung, W.; Halajnia, A.; Lakzian, A.; Kabra, A.N.; Jeon, B.-H. Removal of arsenate and arsenite from aqueous solution by adsorption on clay minerals. *Geosystem. Eng.* **2015**, *18*, 302–311. <https://doi.org/10.1080/12269328.2015.1062436>.
87. Rahman, I.M.M.; Iwakabe, K.; Kawasaki, J. Laterite-a potential alternative for removal of groundwater arsenic. *J. Appl. Sci. Environ. Manag.* **2008**, *12*, 93–100. <https://doi.org/10.4314/jasem.v12i1.55579>.
88. Ho, Y.S.; Mckay, G. Pseudo-second order model for sorption processes. *Process. Biochem.* **1999**, *34*, 451–465. [https://doi.org/10.1016/S0032-9592\(98\)00112-5](https://doi.org/10.1016/S0032-9592(98)00112-5).
89. Saadon, S.A.; Salmiati Yusoff, A.R.M.; Yusop, Z.; Azman, S.; Uy, D.; Syaifiddin, A. Heated laterite as a low-cost adsorbent for arsenic removal from aqueous solution. *Mal. J. Fund. Appl. Sci.* **2018**, *14*, 1–8. <https://doi.org/10.11113/mjfas.v14n1.718>.

90. Mbaye, A.; Diop, C.; Miehe-Brendle, J.; Senocq, F.; Maury, F. Characterization of natural and chemically modified kaolinite from Mako (Senegal) to remove lead from aqueous solutions. *Clay Miner.* **2014**, *49*, 527–539. <https://doi.org/10.1180/claymin.2014.049.4.03>.
91. Russell, J.D.; Fraser, A.R. Infrared methods. In *Clay Mineralogy: Spectroscopic and Chemical Determinative Methods*; Wilson, M.J., Ed.; Springer: Dordrecht, The Netherlands, 1994; pp. 11–67. https://doi.org/10.1007/978-94-011-0727-3_2.
92. Ioannou, A.; Dimirkou, A. Phosphate adsorption on hematite, kaolinite, and kaolinite–hematite (k–h) systems as described by a constant capacitance model. *J. Colloid. Interface Sci.* **1997**, *192*, 119–128. <https://doi.org/10.1006/jcis.1997.4970>.
93. Lan, S.; Zhou, S.; Zhang, Q.; Li, Y.; Yan, Y.; Liang, F.; Jiang, G.; Qin, Z. The effect of proton and arsenic concentration on As(III) removal by hematite and kaolin complexes. *Adsorp. Sci. Technol.* **2021**, *2021*, 3126767. <https://doi.org/10.1155/2021/3126767>.
94. Saikia, N.J.; Bharali, D.J.; Sengupta, P.; Bordoloi, D.; Goswamee, R.L.; Saikia, P.C.; Borthakur, P.C. Characterization, beneficiation and utilization of a kaolinite clay from Assam, India. *Appl. Clay Sci.* **2003**, *24*, 93–103. [https://doi.org/10.1016/S0169-1317\(03\)00151-0](https://doi.org/10.1016/S0169-1317(03)00151-0).
95. Mustapha, S.; Ndamitso, M.M.; Abdulkareem, A.S.; Tijani, J.O.; Mohammed, A.K.; Shuaib, D.T. Potential of using kaolin as a natural adsorbent for the removal of pollutants from tannery wastewater. *Heliyon* **2019**, *5*, e02923. <https://doi.org/10.1016/j.heliyon.2019.e02923>.
96. Bourman, R.P.; Ollier, C.D. A critique of the Schellmann definition and classification of ‘laterite’. *Catena* **2002**, *47*, 117–131. [https://doi.org/10.1016/S0341-8162\(01\)00178-3](https://doi.org/10.1016/S0341-8162(01)00178-3).
97. Nikić, J.; Tubić, A.; Watson, M.; Maletić, S.; Šolić, M.; Majkić, T.; Agbaba, J. Arsenic removal from water by green synthesized magnetic nanoparticles. *Water* **2021**, *11*, 2520. <https://doi.org/10.3390/w11122520>.